ISSN 1070-4272, Russian Journal of Applied Chemistry, 2018, Vol. 91, No. 3, pp. 454−462. © Pleiades Publishing, Ltd., 2018.
Original Russian Text © N.S. Kozhevnikova, O.I. Gyrdasova, I.V. Baklanova, L.Yu. Buldakova, M.Yu. Yanchenko, A.S. Vorokh, 2018, published in Zhurnal Prikladnoi Khimii, 2018, Vol. 91, No. 3, pp. 417−425.

SPECIFIC TECHNOLOGICAL SOLUTIONS

Surface-Modified CdS/ZnO Material: Single-Reactor Synthesis and Mechanism of Formation in Aqueous Solution

N. S. Kozhevnikova*, O. I. Gyrdasova, I. V. Baklanova, L. Yu. Buldakova, M. Yu. Yanchenko, and A. S. Vorokh

Institute of Solid-State Chemistry, Ural Branch, Russian Academy of Sciences, ul. Pervomaiskaya 91, Yekaterinburg, 620990 Russia
**e-mail: kozhevnikova@ihim.uran.ru*

Received January 15, 2018

Abstract—Method of chemical precipitation from aqueous solutions was used to cover the surface of polycrystalline ZnO nanotubes with a nanostructured CdS layer. The thus synthesized CdS/ZnO composite material was studied by the methods of X-ray diffraction analysis, electron microscopy, and optical spectroscopy. The fundamental time-related aspects of the process of CdS formation on the ZnO surface were examined. It was found that the amount of deposited CdS nanoparticles is independent of the deposition duration. The morphological specific features of ZnO nanotubes are preserved upon a prolonged keeping of ZnO in solution. The photocatalytic activity of CdS/ZnO under visible and UV light was examined in the reaction of hydroquinone oxidation. A possible mechanism of how the CdS/ZnO composite is formed in an aqueous solution in the course of growth of a layer constituted by CdS nanoparticles on the surface of ZnO nanotubes is suggested on the basis of the experimental data. It is demonstrated that the chemical-precipitation method can be used to obtain surface-active composite materials that are photoactive in the visible spectral range.

DOI: 10.1134/S1070427218030187

Zinc oxide ZnO belongs to the group of multifunctional wide-bandgap semiconductors and is used in oxidation photocatalysts, gas sensors, voltage-controlled resistors, planar field displays, etc. However, the potential applications of ZnO as a photoactive material are limited to the UV spectral range because of its wide bandgap. It is commonly believed that one of the main ways to extend the spectral range of ZnO sensitivity to longer wavelengths is via its chemical modification (sensitization) with optically active compounds, e.g., chalcogenide nanoparticles (quantum dots, QDs) of CdS, CdSe, CdTe, and PbS [1]. If ZnO has a developed surface, the most effective sensitization variant is to form a thin chalcogenide layer on the surface of the oxide matrix. In contrast to a bulk composite, such a surface-modified material can provide a close and continuous contact of two materials with different energy gap widths (heterojunction). The substantial difference between the energy gap widths of ZnO (3.4 eV [3]) and CdS (2.4 eV [4]) makes the CdS/ZnO composite a promising material for application as a photocatalyst in reactions of oxidation of organic compounds and as a photoabsorbing layer in solar cells.

The goal of our study was to describe processes occurring when the CdS/ZnO composite is formed in an aqueous solution. The composite was synthesized via precipitation of CdS nanoparticles from an aqueous solution onto preliminarily synthesized ZnO nanotubes. The samples were obtained at different synthesis durations and their phase composition, crystal structure, morphology, and optical properties were studied. The mechanism by which CdS nanoparticles are formed on the ZnO surface is suggested on the basis of the data obtained. The photocatalytic activity of the CdS/ZnO composite under visible light was examined in the model reaction of hydroquinone (HQ) oxidation.

EXPERIMENTAL

ZnO nanotubes were synthesized via thermolysis of organic precursors (or by the precursor method) [5. In the first stage, zinc formate $Zn(HCOO)_2 \cdot 2H_2O$ was produced by the action of formic acid on spectral-purity ZnO under heating:

$$ZnO + 2HCOOH + H_2O = Zn(HCOO)_2 \cdot 2H_2O. \quad (1)$$

Then, zinc formatoglycolate $Zn(HCOO) \cdot (OCH_2CH_2O)_{0.5}$ was synthesized at 100°C by the brutto-reaction

$$Zn(HCOO)_2 \cdot 2H_2O + 0.5HOCH_2CH_2OH = Zn(HCOO)(OCH_2CH_2O)_{0.5} + HCOOH\uparrow + 2H_2O. \quad (2)$$

The resulting $Zn(HCOO(OCH_2CH_2O)_{0.5}$ was annealed in air at 500°C for 2 h. The thermolysis of $Zn(HCOO(OCH_2CH_2O)_{0.5}$ yielded ZnO with a quasi-1D morphology of tubular aggregates (nanotubes) and HCP (face-centered close-packed) structure of the wurtzite type (B4) [5].

The ZnO nanotubes were sensitized with CdS nanoparticles, and the surface-modified CdS/ZnO material was produced by the method of chemical precipitation from aqueous solutions. For this purpose, a 0.3-g weighed portion of ZnO was placed in a 250 mL of a solution containing 1.25×10^{-3} mol of cadmium chloride $CdCl_2$, 0.375 mol of aqueous ammonia, and 12.5×10^{-3} mol of thiocarbonic acid diamide N_2H_4CS at initial pH value of 12.73 ± 0.02.

The process of CdS formation in the $CdCl_2$–NH_4OH–$(NH_2)_2CS$ can be represented by the overall equation [4, 6]:

$$Cd(NH_3)_n^{2+} + (NH_2)_2CS + 2OH^- = CdS\downarrow + nNH_3 + H_2NCN + 2H_2O. \quad (3)$$

CdS/ZnO-1, CdS/ZnO-2, and CdS/ZnO-3 samples were precipitated at a temperature of 325 K in the course of 30, 120, and 240 min, respectively. The CdS/ZnO-4 sample was produced by precipitation first at 325 K in the course of 180 min and then at 295 K for 24 h. The equilibrium pH value of the solutions was 13.46 ± 0.04 for all the samples. The constant temperature in the course of reaction (3) was maintained with an LOIP LT-105 liquid thermostat (Russia), with temperature stability within 0.1°. The pH value was monitored with a 150MI pH-meter (Russia) with a combined electrode and measurement accuracy of 0.02 on the pH scale.

To determine the solubility of ZnO nanotubes upon deposition of CdS onto their surface and also to monitor the extent of reaction (3), an elemental analysis of aqueous solutions over the CdS/ZnO deposits for the content of zinc and cadmium atoms was made by the method of atomic-adsorption spectroscopy in an acetylene–air flame on a Perkin Elmer atomic-absorption spectrometer (United States).

The theoretical values of the equilibrium concentration $[Cd^{2+}]_{aq}$ and $[OH^-]_{aq}$ in solution over the $Cd(OH)_2$ and CdS deposits were calculated on the following assumptions: for poorly soluble compounds ($K_{sp} < 10^{-7}$), the ion concentrations in its saturated solution are very low; (b) the saturated solution concentration is such that the activity coefficients of the ions are close to unity, and, consequently, the activities of the ions are nearly equal to their concentrations.

An X-ray diffraction analysis of the composites was made with STADI-P (STOE, Germany) and Shimadzu MAXima-X XRD-7000 Japan) automated X-ray diffractometers with CuK_α radiation, 2θ angle step of 0.03°, and keeping at a point for 10 s. The diffraction patterns were analyzed via full-profile description of a diffraction curve with Multipeak Fit 2 software package with IgorPro 6.1. The phase composition of the samples was evaluated by the partial intensities of reflections associated with separate phases. The particles sizes of various phases were determined by the Scherrer formula $D = \lambda/B \cos\theta$, where D is the size of particles (coherent scattering regions); λ, wavelength of the X-ray radiation; B, full width of a reflection at its half maximum; and θ, radiation incidence angle.

The morphological and microstructural characteristics and the elemental composition of the samples were determined by scanning electron microscopy (SEM) on a JEOL JSM 6390LA electron microscope equipped with a JED-2300 elemental-analysis attachment (Japan). Absorption spectra of pure CdS, ZnO, and CdS/ZnO composites in the visible and UV spectral ranges were obtained with a Shimadzu V-3600 spectrophotometer at wavelengths of 300–700 nm with an integrating sphere and $BaSO_4$ as reference.

Having an energy gap width of 3.4 eV, ZnO has a photocatalytic activity under UV irradiation at wavelengths of less than 370 nm. The tight binding of ZnO and CdS at a surface modification of ZnO

Table 1. Phase composition and particle size of composite samples CdS/ZnO-1–4

Parameter	CdS/ZnO-1	CdS/ZnO-2	CdS/ZnO-3	CdS/ZnO-4
Synthesis duration, min	30	120	240	1620 (27 h)
Phase composition, wt %				
CdS	52.1	52.9	47.4	57.7
ZnO	47.9	46.4	45.8	13.7
$Cd(OH)_2$	0.0	0.7	6.8	20.6
ZnS	–	–	–	8.0
Particle size, nm:				
CdS	5.5	6.4	7.7	5.2
ZnO	23.4	24.1	25.8	32.6
$Cd(OH)_2$	–	16.9	73.0	52.1
ZnS	–	–	–	1.5
Element ratio on the ZnO surface:				
Cd : S	1 : 1	1.6 : 1	1.9 : 1	0.8 : 1
Zn : Cd	8.7 : 1	5.6 : 1	7.6 : 1	83.3 : 1

nanotubes with CdS nanoparticles must give rise to a photocatalytic activity under exposure to visible light. To verify this statement and determine whether there is an electronic contact between CdS nanoparticles and a ZnO nanotube, we evaluated the photocatalytic properties of the CdS/ZnO composite in the visible spectral range by using quinone (component of the hydroquinone/quinone electrochemical pair) with opening of the benzene ring as the argument of the quinone oxidation reaction.

For this purpose, we introduced a 50-mg portion of a sample studied as a photocatalyst into 0.4 mM HQ solutions and exposed the mixture to a UV or visible radiation. The UV irradiation of hydroquinone solutions was performed in quartz electrochemical cells with a BUF-15 lamp (λ_{max} = 253 nm). The oxidation under exposure to a blue lamp (λ_{max} = 440–460 nm) was performed in glass electrochemical cells. The concentration of the substrate being oxidized was measured in discrete intervals of time (1–2 h) by the height of the quinone oxidation peak at 0 V. The amount of HQ in solution was found from the calibration plot by the voltammetric method on a PU-1 polarograph with a three-electrode measurement scheme (glassy carbon indicator electrode, and silver chloride reference and auxiliary electrodes). The potential variation rate in the measurements was constant (0.030 V s^{-1}).

Thus, we performed a set of experiments on HQ oxidation under visible and UV irradiation in the presence of the CdS/ZnO composite. In addition, we performed a set of comparison experiments with pure CdS as a HQ oxidation catalyst under exposure to visible light.

RESULTS AND DISCUSSION

According to XRD data, all the samples contain CdS and ZnO phases, and the $Cd(OH)_2$ phase was found in sample nos. 2–4 (Table 1). The ZnO phase corresponds to the hexagonal structure of wurtzite (space group N196 P63mc) with cell parameters a = 0.325 nm and c = 0.521 nm (PDF N 00-036-1451). Table 1 lists the partial fractions of phases found in the samples and the particle sizes. For example, the fraction of ZnO in sample nos. 1–3 is less than 50% of the total mass. The dependence of the synthesis duration appears only after 27 h, when the content of ZnO substantially falls and reaches 14% in sample no. 4. The size of coherent scattering regions in ZnO varies between 23 and 33 nm. This means that oxide nanotubes are agglomerates of nanoparticles.

The mass fraction of nanostructured CdS in sample nos. 1–3 is about a half of the whole composite and increases to 58% in sample no. 4. The CdS particle size is

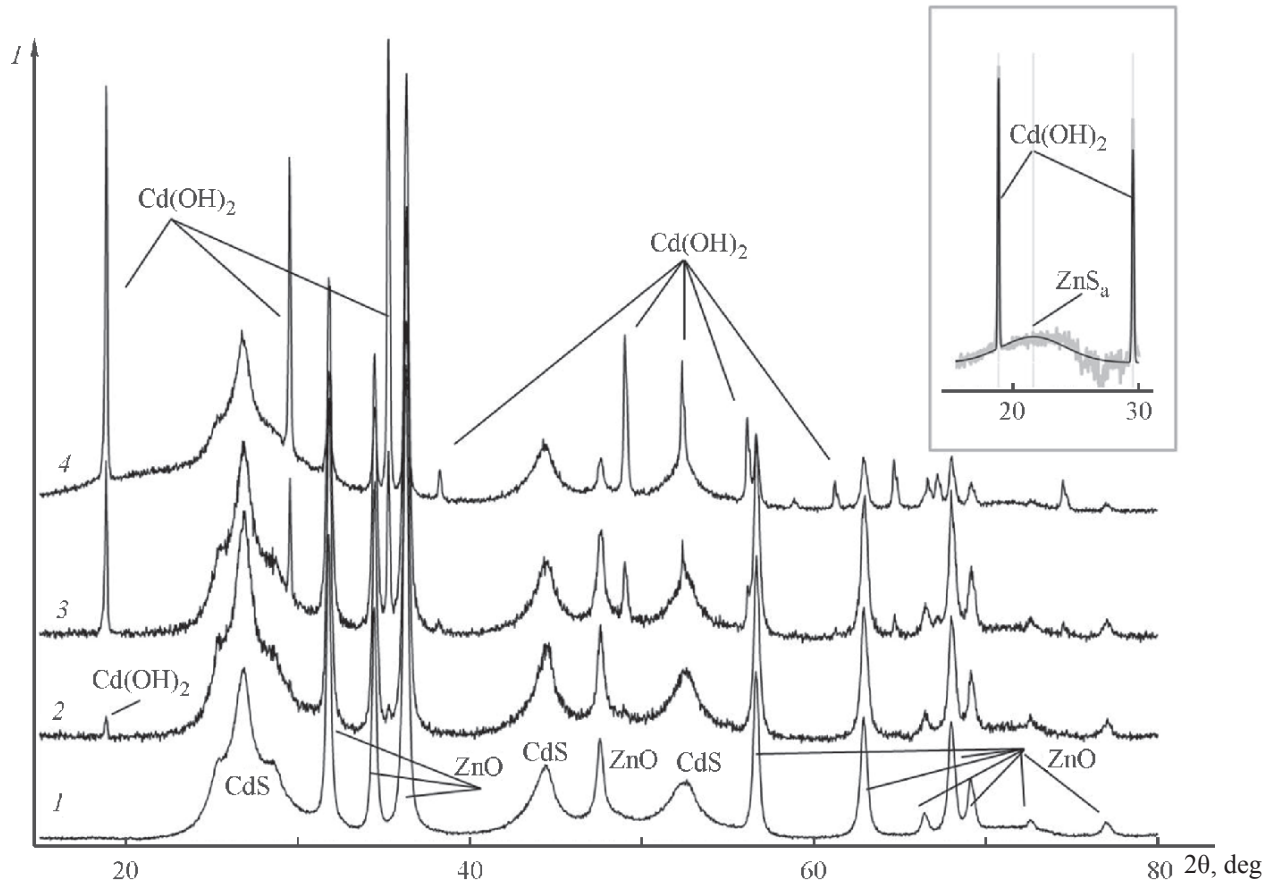

Fig. 1. X-ray diffraction patterns of CdS/ZnO-1–4 samples. (*I*) Intensity and (2θ) Bragg angle.

actually independent of time and constitutes about 5–8 nm. The crystal structure of CdS is determined from three reflections at 2θ angles in the range from 10 to 55° at 26.7, 44, and 52° and has the form of a random close packing. This CdS structure is described by an "averaged lattice" with hexagonal (space group N 168 P6) symmetry and unit cell parameters $a = 0.236$ nm and $c = 0.334$ nm. Here, a is the distance between projections of all atoms on the packing plane, and c is the distance between the nearest close-packed layers with like atoms (Cd or S) [7].

The third phase $Cd(OH)_2$ appears only after 30 min of synthesis (sample no. 2), being formed in an insignificant amount (< 1%). In this stage, the phase is identified by the reflection [001], $2\theta = 18.9°$. After 4 h of synthesis (sample nos. 3 and 4), there appear rest of the reflections characteristic of $Cd(OH)_2$. The layered structure of $Cd(OH)_2$ is described by a hexagonal lattice (space group N 164 P3m1) and cell parameters $a = 0.349$ nm and $c = 0.471$ nm (PDF N 00-031-0228). $Cd(OH)_2$ layersare bound together by van der Waals bonds. The [001] direction is perpendicular to the packing layers. The rise in the intensity of the [001] reflection in the first stage reflects the growth of particles predominantly along this axis, i.e., via formation of new $Cd(OH)_2$ layers. In the course of time, the fraction of $Cd(OH)_2$ grows, other reflections appear, and the relative intensities of various reflections become level. These data suggest that, in 4 h, hydroxide particles grow in all the crystallographic directions.

In addition, the diffraction pattern of sample no. 4 shows a halo at angles $2\theta = 15–30°$, which indicates that the amorphous phase is formed after 24 h of synthesis. The inset of Fig. 1 shows a fragment of the difference spectrum between the diffraction patterns of sample nos. 3 and 4 and its decomposition into separate reflections. The narrow reflections correspond to coarsely crystalline $Cd(OH)_2$, and the broad peak can be attributed to the ZnS phase. The formation of the ZnS phase is due to the decomposition of ZnO, which is confirmed

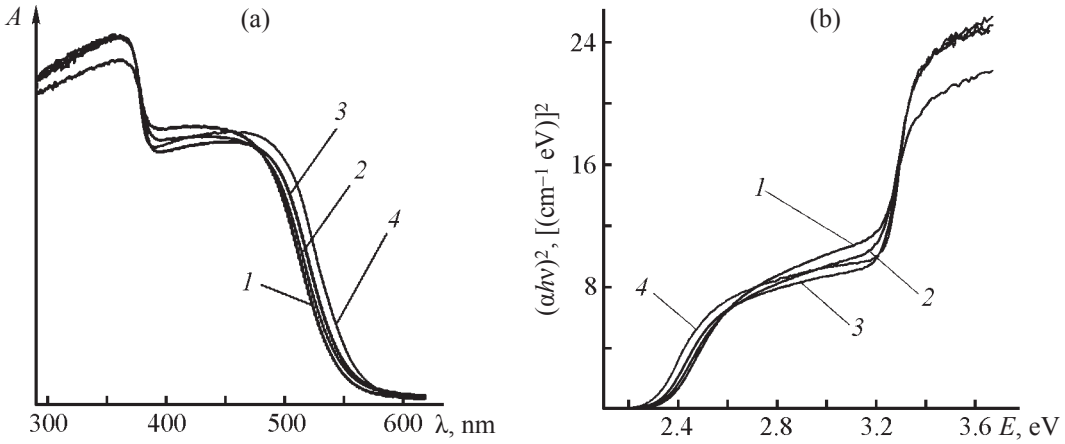

Fig. 2. (a) Absorption (A) spectra in the UV and visible spectral ranges and (b) determination of the effective energy gap width of composite CdS/ZnO-1–4 samples produced in (*1*) 30, (*2*) 120, (*3*) 240 min, and (*4*) 24 h after the beginning of synthesis. (λ) Wavelength, $[(\alpha h\nu)_2]$ squared product of the absorption coefficient α by the photon energy *h*ν, and (*E*) energy.

by the decrease in the mass fraction of ZnO according to XRD data (Table 1). According to these data, the partial contribution of ZnS in the composite is 8%. The size of the coherent scattering regions of the ZnS phase is 1.5 nm.

Figure 2 shows absorption spectra in the UV and visible ranges for CdS/ZnO composites. The spectra show two absorption edges, from ZnO nanotubes and CdS nanoparticles, which confirms the presence of these two phases in the samples synthesized. The presence of the third phase, $Cd(OH)_2$, could not be confirmed by optical measurements because the energy gap of $Cd(OH)_2$ is about 4.5 eV [8], and, accordingly,

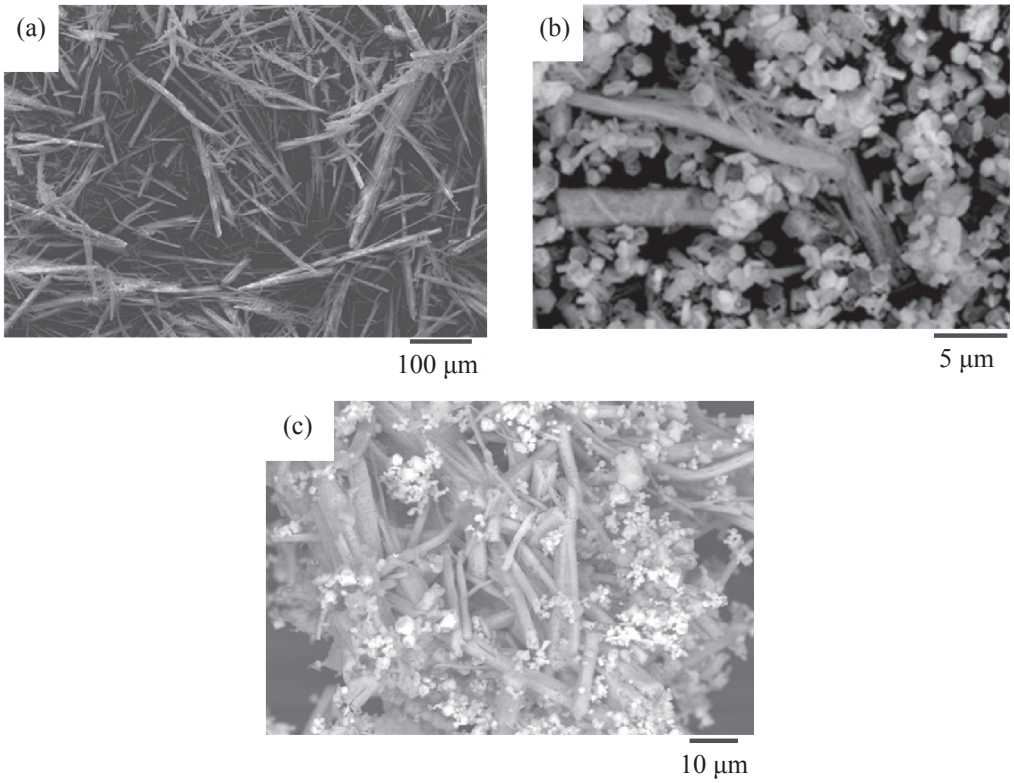

Fig. 3. SEM micrographs of (a) and the change of the microstructure of CdS/ZnO composite samples obtained after (b) 240 min and (c) 24 h of synthesis.

Table 2. Solubility of ZnO nanotubes and extent of the reaction in which CdS particles are produced in formation of CdS/ZnO composite samples

Sample	Metal concentration in solution after the end of synthesis, M		Amount of ZnO that passed into solution, mol %	Conversion of cadmium ions to a solid phase
	Zn	Cd		
CdS/ZnO-1	0.0021	3.5×10^{-6}	14	0.9993
CdS/ZnO-2	0.0024	9×10^{-8}	16	0.999994
CdS/ZnO-3	0.0024	9×10^{-8}	17	→ 1
CdS/ZnO-4	0.0012	$\leq 9 \times 10^{-8}$	16	→ 1

the absorption edge of $Cd(OH)_2$ at around 270 nm lies outside the range of our measurements.

To determine the effective energy gap width of CdSZnO, the experimental spectra were brought to the form $(\alpha h\nu)^2 = f(h\nu)$. The frequency dependence of the absorption coefficient near the absorption edge is described by the following equation:

$$\alpha(\nu) = [A(h\nu - E_g)^{1/2}]/h\nu,$$

where α is the absorption coefficient; $h\nu$, photon energy; E_g, optical gap width; and A, constant independent of the frequency ν [8].

The extrapolation of the linear portions of the resulting curves to intersection with the abscissa axis was used to determine the energy gap widths. E_g determined for ZnO by the procedure described in [9] remains nearly constant (3.10 eV) in sample nos. 1–4. However, a long-wavelength shift of the absorption edge of CdS nanoparticles is observed in CdS/ZnO composites relative to the coarsely crystalline CdS (2.40 eV). The energy gap width of CdS nanoparticles in sample nos. 1–4 slightly decreases with increasing precipitation duration and is 2.36, 2.35, 2.33, and 2.30 eV, respectively (the E_g measurement error does not exceed 5×10^{-3} eV). According to the XRD data (Table 1), the size of CdS nanoparticles is nearly independent of the synthesis duration, and, consequently, does not affect the value of E_g. The variation of E_g is probably due to the decrease in the fraction of surface CdS atoms in the course of interaction with the oxide ZnO matrix [4, 10].

According to SEM data (Fig. 3), ZnO retains in the course of sensitization the initial size and shape of tubular aggregates. The micrographs of sample nos. 3 and 4 (Figs. 2b and 2c) show agglomerates having the regular shape of a hexagonal prism, with the number of these growing in the course of time. It has been shown [4] that this shape is inherent in $Cd(OH)_2$ crystals. The results of XRD and chemical analyses of the composites and a quantitative analysis of the ionic composition of the solution over the precipitates also indicate that agglomerates of regular shape belong to the $Cd(OH)_2$ crystal phase with minor content of CdS. The CdS phase is poorly seen in the micrographs (Figs. 3b and 3c) because of the small size of CdS particles. A study of the surface morphology of CdS/ZnO composites, with the elemental composition determined by SEM, made it possible to trace how the Cd : S and Zn : Cd element ratios vary in the course of time (Table 1).

An elemental analysis of aqueous solutions over the CdS/ZnO deposits demonstrated that the solubility of ZnO nanotubes upon the deposition of CdS on their surface does not exceed 17 mol %, and the conversion of $CdCl_2$ to the solid phase reaches a value of 0.9993 already by 30th minute of precipitation and then remains nearly constant (Table 2). (The degree of conversion is the ratio between the number of moles of *i*th substance that entered into the reaction and the initial number of moles of this substance.)

The results of a photocatalytic oxidation of HQ in the presence of the CdS/ZnO composite (for the example of CdS/ZnO-1 sample) are presented in Fig. 4. The photocatalytic data demonstrate that the HQ concentration in solution in the presence of both CdS/ZnO and pure CdS as catalysts falls in the course of time in comparison with a pure HQ solution without a catalyst.

The activity of the CdS/ZnO composite during the first hours is higher under the UV irradiation, compared with the exposure to visible light. The reason is that,

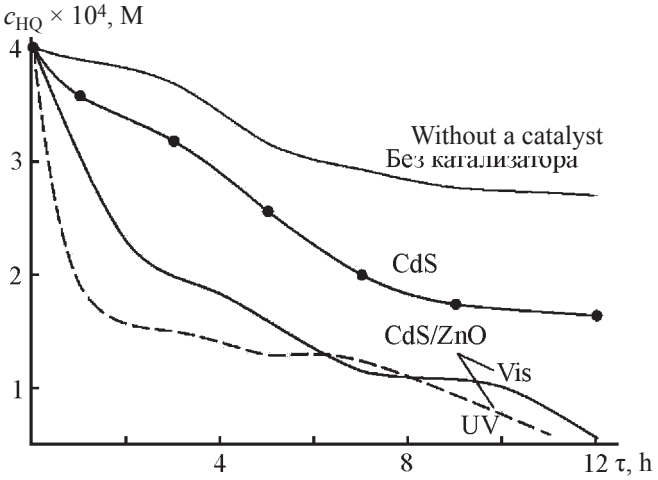

Fig. 4. Results of a photocatalytic oxidation of HQ in the presence of CdS/ZnO (sample 1) undervisible (curve Vis) and UV irradiation (curve UV). For comparison, the figure shows HQ oxidation curves without a catalyst and in the presence of pure CdS under visible irradiation at wavelengths in the range 440–460 nm. (c_{HQ}) Content of hydroquinone and (τ) time.

having a wide energy gap (3.4 eV), the ZnO matrix exhibits photoactivity under the action of UV light, whereas in the visible light, only CdS is active. The difference between the HQ decomposition curves under visible and UV irradiation in the presence of CdS/ZnO confirms the existence of an electronic contact between sulfide nanoparticles and the oxide matrix. In turn, it can be seen in Fig. 4 that using the CdS/ZnO composite instead of the pure optically active CdS makes substantially larger the extent of the reaction of quinone oxidation under irradiation with visible light. Thus, the deposition of photoactive CdS nanoparticles onto the semiconducting matrix can raise the photocatalytic activity of the composite material in the visible light.

Based on the experimental data, we can distinguish three processes occurring in solution when the CdS/ZnO composite is formed.

(1) Formation of CdS nanoparticles in solution and deposition of CdS onto ZnO nanotubes. During the first 30 min of the ZnO sensitization process, N_2H_4CS molecules are hydrolyzed by a reversible reaction to give S^{2-} ions [4, 6, 11]:

$$SC(NH_2)_2 \leftrightarrows H_2S + H_2CN_2, \quad (4)$$

which are directly involved in the formation of CdS by Eq. 3). During this time, the amount of CdS in the CdS/ZnO composite reaches ~50 wt % (sample no. 1) and remains nearly constant in sample nos. 2–4. The Cd : S element ratio in sample no. 1 is 1 : 1 (Table 1), which corresponds to the CdS phase and agrees with the XRD data.

The experimentally determined concentration of free and complex ions, Cd^{2+} and $Cd(NH_3)_n^{2+}$, in solution over the CdS/ZnO composite, $c_{CD,aq}$, was 3.5×10^{-6} M by the 30th minute of synthesis (Table 2), which substantially exceeds the theoretical equilibrium value $[Cd^{2+}]_{aq}/CdS = 8.89 \times 10^{-14}$ M calculated from the solubility product $K_{sp}(CdS) = 7.9 \times 10^{-27}$ [12]. This means that, theoretically, CdS nanoparticles must continue to be formed and(or) grow in solution.

According to the XRD data, the mass fraction and size of CdS particles do not vary with time, which shows that the CdS concentration in sample nos. 2–4 is constant and reactions (3) and (4) stop after 30 min of synthesis. Because the value of $c_{Cd,aq}$ remains comparatively high by 30th minute of synthesis and does not hinder the formation of CdS, the termination of reaction (3) is due to the absence of a source of S^{2-}, thiourea N_2H_4CS. Probably, the large specific surface area of ZnO nanotubes results in that, after 30 min of synthesis, part of N_2H_4CS molecules starts to be sorbed on the tubes to give surface complexes of the type $Zn[N_2H_4CS]_n$ [13], with the concentration of N_2H_4CS molecules and, accordingly, S^{2-} ions in solution dramatically reduced.

Thus, a solid nanocrystalline CdS phase is formed during the first 30 min of synthesis [Eq. (3)] and deposited onto the ZnO surface, with the thiourea adsorption beginning (Fig. 5)

(2) Formation of $Cd(OH)_2$ particles. It can be seen in Table 2, that the concentration $c_{Cd,aq}$ decreases by 120th minute of synthesis and one more solid phase, $Cd(OH)_2$, starts to be formed (less than 1 wt % in sample CdS/ZnO-2) (Table 1). This process continues during a long time and the amount of $Cd(OH)_2$ reaches a significant value (21 wt %) in sample no. 4. It is important to note that, during the first hours, the mass fraction of $Cd(OH)_2$ grows simultaneously with the particle size, which increases from 17 to 73 nm, but this correlation disappears after 24 h. It can be stated that, during the first hours, the $Cd(OH)_2$ phase predominantly grows due to the growth of the already formed crystals, whereas after 4 h, the number of nuclei starts to increase.

To explain the observed formation of a new solid phase $Cd(OH)_2$, we calculated the theoretical concentration $[Cd^{2+}]_{aq/Cd(OH)2}$ in a saturated solution

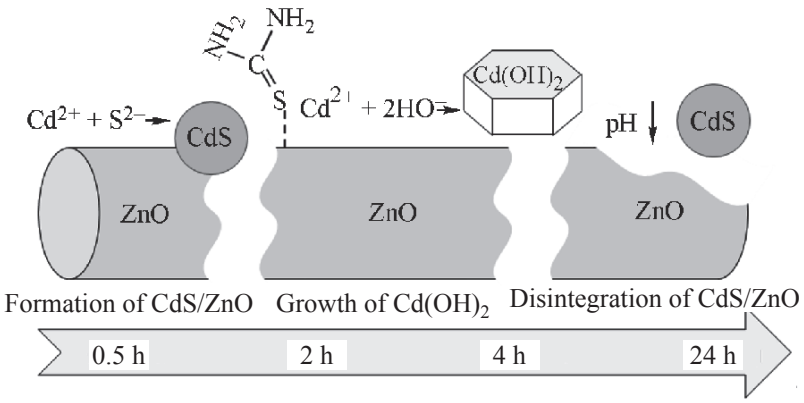

Fig. 5. Mechanism by which surface-modified CdS/ZnO material is formed in an aqueous solution.

over the $Cd(OH)_2$ deposit at which $Cd(OH)_2$ can be formed. $[Cd^{2+}]_{aq/Cd(OH)_2}$ was calculated from data on the solubility product $K_{sp}[Cd(OH)_2] = 2.2 \times 10^{-14}$ [11] with consideration for the presence in solution of a strong NaOH electrolyte containing the same anion. At pH 12.73, $[Cd^{2+}]_{aq/Cd(OH)_2}$ is 7.6×10^{-14} 10^{-12} M, which is several orders of magnitude smaller than the experimental value $c_{Cd,aq} = 9 \times 10^{-14}10^{-8}$ M (Table 2). Thus, the concentration of hydroxide ions at pH ≥ 12.7 is sufficient for reaching $K_{sp}[Cd(OH)_2]$, and Cd^{2+} and $Cd(NH_3)_n^{2+}$ ions start to interact with OH^- ions, which leads to the nucleation and the subsequent crystallization of the $Cd(OH)_2$ phase directly in solution:

$$Cd^{2+}/Cd(NH_3)_n^{2+} + 2OH^- = Cd(OH)_2\downarrow + nNH_3. \quad (5)$$

However, reaction (5) does not reduce the concentration $c_{Cd,aq}$ (Table 2). The constant-in-time value of $c_{Cd,aq}$ (Table 2) in a solution over the sample nos. 2–4, rather slow (during 24 h) growth of $Cd(OH)_2$, and appearance of an excess amount of cadmium atoms (relative to sulfur atoms) on the surface of ZnO nanotubes (Table 1) in sample nos. 2 and 3 suggest that also possible in sensitization of ZnO, together with the chemical reactions in which CdS [reaction (3)] and $Cd(OH)_2$ [reaction (5)] are formed, is the sorption of free Cd^{2+} and complex $Cd(NH_3)_n^{2+}$ ions on the developed surface of ZnO nanotubes. It is the sorption that leads to a decrease in $c_{Cd,aq}$ after 30 min of synthesis, and its dynamic nature maintains $c_{Cd,aq}$ constant after 120 min of synthesis and supports the slow growth of $Cd(OH)_2$ particles. Taking into account the aforesaid, we can represent the process of $Cd(OH)_2$ formation as follows:

$$ZnO_{solid} + Cd^{2+}/Cd(NH_3)_n^{2+} \rightarrow [Cd^{2+}/Cd(NH_3)_n^{2+}]_{ads/ZnO},$$

$$[Cd^{2+}/Cd(NH_3)_n^{2+}]_{ads/ZnO} \quad [Cd^{2+}/Cd(NH_3)_n^{2+}]_{aq},$$

$$[Cd^{2+}/Cd(NH_3)_n^{2+}]_{aq} + 2OH^- = Cd(OH)_2\downarrow + nNH_3.$$

Thus, by the 120th minute of synthesis of the CdS/ZnO composite (Fig. 5), the formation of CdS nanoparticles in solution ends due to the sharp decrease in the concentration of sulfidizer, N_2H_4CS, and particles of the $Cd(OH)_2$ solid phase start to be formed and grow, which is accompanied by the sorption of free Cd^{2+} and complex $Cd(NH_3)_n^{2+}$ ions on the ZnO surface.

(3) Disintegration of the CdS/ZnO composite and formation of the amorphous ZnS phase. Upon a prolonged keeping of the CdS/ZnO composite (sample no. 4) in an alkaline solution, the mass fraction of ZnO in the composite becomes three times smaller (14 wt %), and the quantitative element ratio Cd : S becomes nearly stoichiometric (Table 1). This is indicative of the degradation onset of the composite: ZnO starts to dissolve, the surface of a ZnO nanotube disintegrates, and CdS nanoparticles are desorbed from the ZnO surface. In the process, the morphology of the tubular ZnO aggregates is preserved (Fig. 2c). Analysis of the diffraction patterns of sample no. 4 (Fig. 1) demonstrates that one more phase appears, amorphous zinc sulfide ZnS. The reaction in which ZnS is formed in an aqueous solution containing thiourea and ammonia can be represented as

$$ZnO_{solid} \rightarrow Zn\ ZnO_{sol}\cdot H_2O\ \ Zn^{2+} + 2OH^-,$$

$$Zn(NH_3)_n^{2+} + (NH_2)_2CS + 2OH^-$$

$$= ZnS\downarrow + nNH_3 + H_2NCN + 2H_2O \quad (6)$$

CONCLUSIONS

The sensitization of ZnO nanotubes with CdS nanoparticles by the method of chemical precipitation from solution yields a CdS/ZnO composite material. The amount of deposited CdS nanoparticles is independent of the precipitation duration. In the case of a prolonged keeping of ZnO nanotubes in solution, the morphological features of the polycrystalline nanotubes are preserved. At the same time, a prolonged keeping in solution causes a gradual degradation of the oxide matrix, which changes the phase composition of the composite and leads to nucleation and growth of particles of the $Cd(OH)_2$ phase. The results obtained make it possible to synthesize a CdS/ZnO composite with prescribed characteristics related to the composition and optical properties. The composite exhibits a catalytic activity in the visible spectral range, which confirms the possibility of its effective use as a photocatalyst and absorbing layer of a solar cell.

ACKNOWLEDGMENTS

The study was supported by the Russian Science Foundation (project no. 17-79-20165).

REFERENCES

1. Troshyn, O.V., Kovalenko, A.A., Dorofeev, S.G., and Baranov, A.N., *Inorg. Mater.,* 2012, vol. 48, no. 7, pp. 709–715.
2. Lisichkin, G.V., Fadeev, A.Yu., Serdan, A.A., et al., *Khimiya privitykh poverkhnostnykh soedinenii* (Chemistry of Grafted Surface Compounds), Lisichkin, G.V., Ed., Moscow: Fizmatlit, 2003.
3. Park, C.H., Zhang, S.B, and Wei, S.-H., *Phys. Rev. B*, 2002, vol. 66, no. 15, p. 073202.
4. Kozhevnikova, N.S.,Vorokh, A.S., and Uritskaya, A.A., *Russ. Chem. Rev*., 2015, vol. 84, no. 3, pp. 225–250.
5. Shalaeva, E.V., Gyrdasova, O.I., Krasilnikov, V.N., et al., *Nanocomposites, Nanophotonics, Nanobiotechnology, and Applications, Springer Proc. Phys*., 2015, vol. 156, part 26, pp. 313–335.
6. Uritskaya, A.A., Kitaev, G.A., and Belova, N.S., *Russ. J. Appl. Chem*., 2002, vol. 75, no. 5, pp. 846–848.
7. Vorokh, A.S. and Rempel, A.A., *JETP Lett*., 2010, vol. 91, no. 2, pp. 100–104.
8. Zhang, D.E., Pan, X.D., Zhu, H., et al., *Nanoscale Res. Lett*., 2008, no. 3, pp. 284–288.
9. Ukhanov, Yu.I., *Opticheskie svoistva poluprovodnikov* (Optical Properties of Semiconductors), Moscow: Nauka, 1977.
10. Ekimov, A.I. and Onushchenko, A.A., *JETP Lett.,* 1984, vol. 40, no. 8, pp. 1136–1139.
11. Markov, V.F., Maskaeva, L.N., and Ivanov, P.N., *Gidrokhimicheskoe osazhdenie plenok sul'fidov metallov: modelirovanie i eksperiment* (Hydrochemical Deposition of Metal Sulfide Films: Simulation and Experiment), Yekaterinburg: Izd. Ural. Otd. Ross. Akad. Nauk, 2006.
12. Lur'e, Yu.Yu., *Spravochnik po analiticheskoi khimii* (Handbook of Analytical Chemistry), Moscow: Khimiya, 1971.
13. Naymov, A.V., Semenov, V.N., Bolgova, T.G., and Sergeeva, A.V., Proc. *Voronezh State Univ., Chem., Biol., Pharm.*, 2005, vol. 1, pp. 66–68.